Inorganic Chemistry

Article

pubs.acs.org/IC

Synthesis and Characterization of Functionalized *meso*-Triaryltetrabenzocorroles

Giuseppe Pomarico,[†] Sara Nardis,[†] Manuela Stefanelli,[†] Daniel O. Cicero,[†] M. Graça H. Vicente,[‡] Yuanyuan Fang,[§] Ping Chen,[§] Karl M. Kadish,*[,§] and Roberto Paolesse*[,†,⊥]

[†]Dipartimento di Scienze e Tecnologie Chimiche, Università di Roma Tor Vergata, via della Ricerca Scientifica, 1, 00133 Rome, Italy

[‡]Department of Chemistry, Louisiana State University, Baton Rouge, Louisiana 70803, United States

[§]Department of Chemistry, University of Houston, Houston, Texas, 77204-5003 United States

[⊥]CNR IDASC, via Fosso del Cavaliere, 00133 Rome, Italy

Supporting Information

ABSTRACT: 5,10,15-Triaryltetrabenzocorroles functionalized with different electron-withdrawing groups on the *β*,*β*′-fused rings have been prepared by a cross-coupling Heck procedure between octabrominated copper corrole and a terminal alkene bearing electron-withdrawing moieties. The spectroscopic characterization of these complexes showed red-shifted UV−vis absorption bands characterized by a significant band broadening. The same feature was observed in the case of NMR spectra, where low-resolution groups of signals were observed. This behavior derives from a strong tendency of these macrocycles to aggregate in solution, as has been demonstrated by an ^{1}H NMR study performed on one of these tetrabenzocorroles. The influence of the substituents on the fused benzene ring on the properties of the tetrabenzocorroles was investigated by electrochemistry and spectroelectrochemistry, and comparisons were made between properties of the newly synthesized compounds and those of the tetrabenzocorroles reported earlier in the literature.

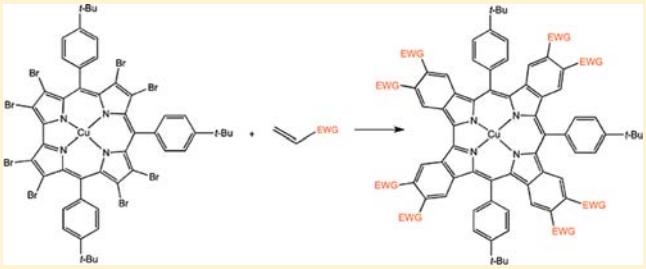

INTRODUCTION

Corrole is a tetrapyrrolic macrocycle, which differs from naturally-occurring porphyrin rings in lacking one *meso* carbon, which is replaced by a direct pyrrole−pyrrole link. Despite this difference in the molecular skeleton, corroles retain an 18-electron *π* aromatic system similar to that of porphyrins. Although corroles are not found in biological systems, the number of investigations of these compounds in the area of synthesis and applications has increased significantly over the past decade and has reached a point where the popularity of studying corroles is in some cases approaching that of the related porphyrins.

After the first report of corrole preparation by Johnson and Kay in 1965,[1] the chemistry of this porphyrinoid stood largely unexplored for several decades; this was mainly due to the difficult multistep procedure originally needed to prepare the precursors that lead to the formation of *β*-alkylcorroles. This situation changed in 1999, when two different synthetic routes for the preparation of *meso*-triarylcorroles starting from commercially available precursors were independently reported in seminal papers from the groups of Gross[2] and Paolesse.[3] Further development of new methods for the large-scale preparation of a wide range of *meso*-triarylcorroles[4−6] allowed for more accurate investigations of the properties of this macrocycle[7−9] and their concomitant use in various fields of research ranging from medicine to sensors to material chemistry.[10−12]

This progress led to the possibility of tuning the properties of corroles by peripheral functionalization, following an approach successfully used in the case of porphyrins, with one end goal being the expanded use of these macrocycles in different applications ranging from catalysis to photovoltaic cells. One interesting modification of the corrole is to expand the aromatic system by introduction of fused rings at the *β*,*β*′-pyrrole positions of the macrocycle. This modification is generally known as annulation and can result in significant variations of the macrocycle photochemical features.

A number of porphyrinoids have been obtained by the introduction of different aromatic rings onto the macrocycle, including benzene,[13] naphthalene,[14] anthracene,[15] phenanthrene,[16] and acenaphthalene.[17] The most common derivatives among these *π*-extended macrocycles are the benzoporphyrins, which show different optical features compared with those of the starting materials;[18,19] for example, there are substantial red shifts of the Soret and Q bands, the latter of which often exhibit increased extinction coefficients. These variations are interest-

Received: April 26, 2013
Revised: June 26, 2013
Accepted: June 26, 2013
Published: July 5, 2013

   dx.doi.org/10.1021/ic4010467 | *Inorg. Chem.* 2013, 52, 8834−8844

Scheme 1. Synthetic Pathway for the Preparation of Cu−Triaryltetrabenzocorrolates by the Cross-Coupling Methodology

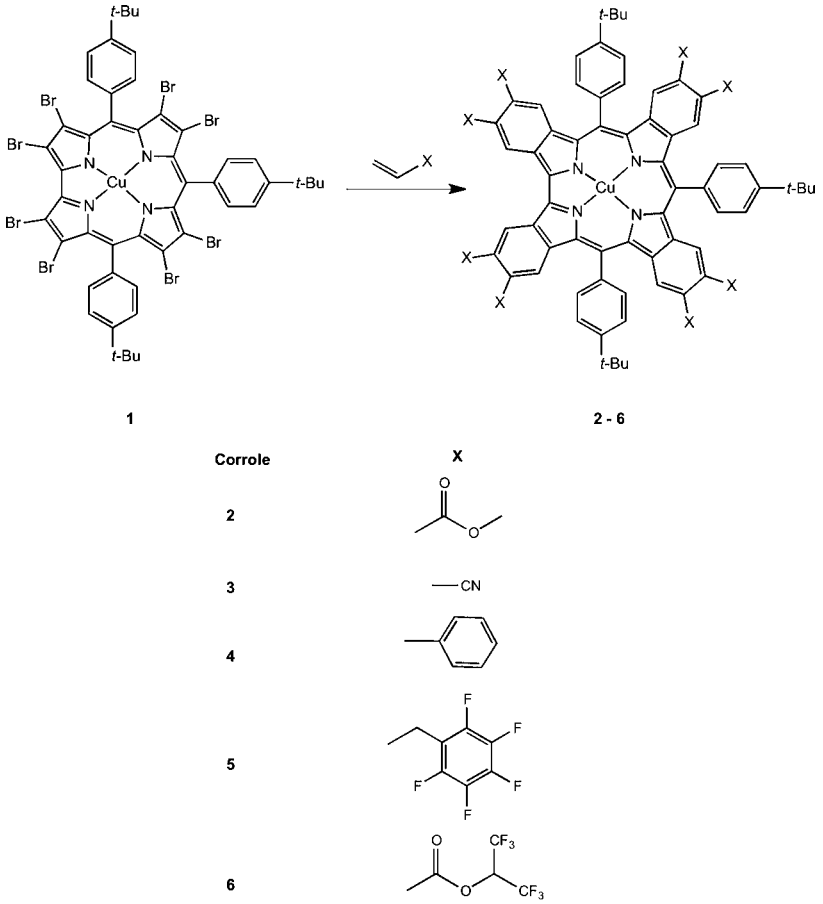

ing for the exploitation of these compounds in several fields of research.

We have been interested in the study of the effect of aromatic ring annulation to the corrole macrocycle and reported the first preparation of a *meso*-triaryltetrabenzocorrole,[20] which was obtained by two different synthetic routes that were previously exploited to obtain analogous tetrabenzoporphyrins.[21,22] One method was based on the condensation of an arylaldehyde with tetrahydroisoindole, a suitable pyrrole bearing a six-membered ring as precursor of the annulated benzene ring. Higher yields of the target corroles were achieved with an alternative synthetic route, shown in Scheme 1, based on a cross-coupling reaction between a brominated copper corrole precursor and methyl acrylate under Heck conditions. The tetrabenzocorroles obtained by this method are characterized by large red shifts of the absorption bands as a result of the extended aromatic system.

Following the discovery of an efficient synthetic pathway for the preparation of triaryltetrabenzocorroles, we investigated the coordination of different metal ions in the core of the macrocycle (Al, Ga, Ge, Cu, P) and the associated axial ligands.[23] Noteworthy results were obtained for the phosphorus complex, which showed the highest fluorescence quantum yield (0.31 in toluene). The potential applications of this type of compound as an optical sensor, a fluorophore in bioimaging, or a singlet oxygen sensitizer in photodynamic therapy, warrant their further syntheses and investigation.

In the present study, we report the preparation of new tetrabenzocorroles containing different electron-withdrawing groups on the fused benzene rings. These modified tetrabenzocorroles were prepared by Heck cross-coupling reactions between the octabromocorrole **1** and terminal olefins bearing different functional groups. We also describe the electrochemical properties of these new compounds.

EXPERIMENTAL SECTION

Materials. Silica gel 60 (70−230 mesh, Sigma Aldrich) was used for column chromatography. Reagents and solvents (Aldrich, Fluka) were HPLC-grade and were used without further purification. ^{1}H spectra were recorded on a Bruker AV300 spectrometer operating at 300.13 MHz. Chemical shifts are given in parts per million relative to residual solvent (7.26 ppm for $CHCl_3$ or 5.32 ppm for CH_2Cl_2). UV−vis spectra were measured in CH_2Cl_2 with a Varian Cary 50 spectrophotometer. IR spectra were recorded in $CHCl_3$ solutions with a Perkin-Elmer 100 FT-IR spectrometer using KBr cells. Mass spectra (TOF-SIMS) were recorded using positive method with TOFSIMS V (IONTOF) spectrometer or (FAB mode) on a VGQuattro spectrometer in the positive ion mode using *m*-nitrobenzyl alcohol (Aldrich) as a matrix.

General Procedure for [Triaryltetrabenzocorrolato]Cu Synthesis. Octabrominated copper corrole **1** (140 mg, 0.101 mmol), $Pd(AcO)_2$ (23.0 mg, 0.101 mmol, 1 equiv), PPh_3 (69.0 mg, 0.264 mmol, 2.62 equiv), K_2CO_3 (120 mg, 0.870 mmol, 8.57 equiv), and EWG-alkene (100-fold excess) were dissolved in a mix of anhydrous toluene/DMF (22 + 15 mL) in a Schlenk tube under nitrogen. The mixture was then degassed via five freeze−pump−thaw cycles before the vessel was purged with nitrogen, sealed, and heated at 125 °C for 72 h. The solvent was removed under reduced pressure and the residue was purified as described below.

dx.doi.org/10.1021/ic4010467 | *Inorg. Chem.* 2013, 52, 8834−8844

[5,10,15-Tris(4-tert-butylphenyl)-2:3,7:8,12:13,17:18-tetrabenzo-2″,3″,7″,8″,12″,13″,17″,18″-octacarboxymethylcorrolato]Cu, [CH_3CO_2-TBC]Cu, ***2***. This was prepared as previously reported.[20]

[5,10,15-Tris(4-tert-butylphenyl)-2:3,7:8,12:13,17:18-tetrabenzo-2″,3″,7″,8″,12″,13″,17″,18″-octacyanocorrolato]Cu, [CN-TBC]Cu, ***3***. The residue was purified by chromatography on silica gel eluted with 2% CH_3OH in CH_2Cl_2, followed by crystallization from CH_2Cl_2/hexane, to afford the desired product. Yield: 22% (26 mg). Mp > 300 °C. UV−vis (CH_2Cl_2) λ_{max}, nm (log ε): 474 (4.72), 605 (3.92), 686 (3.69). IR ($CHCl_3$): 2228 cm^{-1} (CN). ^1H NMR (300.13 MHz, $CDCl_3$): δ 7.71−7.50 (m, 20 H, β-fused + phenyls), 1.44 (br s, 27 H, *tert*-butyls). MS (FAB, *m*/*z*): 1154 (M^+); 1094 (M^+ − Cu). Anal. Calcd for $C_{73}H_{47}CuN_{12}$: C, 75.86; H, 4.10; N, 14.54%. Found: C, 75.81; H, 4.13; N, 14.48%.

[5,10,15-Tris(4-tert-butylphenyl)-2:3,7:8,12:13,17:18-tetrabenzo-2″,3″,7″,8″,12″,13″,17″,18″-octaphenylcorrolato]Cu, [Ph-TBC]Cu, ***4***. The residue was purified by chromatography on silica gel eluted with CH_2Cl_2/hexane (2:1), followed by crystallization from CH_2Cl_2/CH_3OH, to afford the desired product. Yield: 21% (33 mg). Mp > 300 °C. UV−vis (CH_2Cl_2) λ_{max}, nm (log ε): 475 (4.92), 606 (4.17). ^1H NMR (300.13 MHz, CD_2Cl_2): δ 7.61−6.68 (m, 60 H, β-fused + *meso*-phenyls + δ,δ'-phenyls), 1.49−1.33 (m, 27 H, *tert*-butyls). MS (FAB, *m*/*z*): 1564 (M^+). Anal. Calcd for $C_{113}H_{87}CuN_4$: C, 86.75; H, 5.60; N, 3.58%. Found: C, 86.69; H, 5.56; N, 3.53%.

[5,10,15-Tris(4-tert-butylphenyl)-2:3,7:8,12:13,17:18-tetrabenzo-2″,3″,7″,8″,12″,13″,17″,18″-octakis(2,3,4,5,6-pentafluorophenylmethyl)corrolato]Cu, [F_5PhCH_2-TBC]Cu, ***5***. The residue was purified by chromatography on silica gel eluted with CH_2Cl_2/hexane (1:1), to afford the desired product. Yield: 21% (51 mg). Mp > 300 °C. UV−vis (CH_2Cl_2) λ_{max}, nm (log ε): 454 (4.55), 608 (4.08). ^1H NMR (300.13 MHz, $CDCl_3$): δ 7.63−7.34 (m, 20 H, β-fused + phenyls), 3.53−3.47 (m, 16 H, $-CH_2F_5Ph$), 1.41 (br s, 27 H, *tert*-butyls). MS (TOF-SIMS, *m*/*z*): 2396.34 (M^+). Anal. Calcd for $C_{121}H_{63}CuF_{40}N_4$: C, 60.65; H, 2.65; N, 2.34%. Found: C, 60.72; H, 2.60; N, 2.28%.

[5,10,15-Tris(4-tert-butylphenyl)-2:3,7:8,12:13,17:18-tetrabenzo-2″,3″,7″,8″,12″,13″,17″,18″-octacarboxy-(1,1,1,3,3,3,-hexafluoroisopropyl)corrolato]Cu, [IsoF$_6$-TBC]Cu, ***6***. The residue was purified by chromatography on silica gel eluted with CH_2Cl_2/hexane (1:1), to afford the desired product. Yield: 24% (61 mg). Mp > 300 °C. UV−vis (CH_2Cl_2) λ_{max}, nm (log ε): 498 (4.85), 620 (4.11). ^1H NMR (300.13 MHz, $CDCl_3$): δ 7.63−7.33 (br m, 20 H, β-fused + phenyls), 5.98−5.76 (br m, 8 H, $-CO_2CH(CF_3)_2$), 1.45−1.39 (m, 27 H, *tert*-butyls). MS (TOF-SIMS, *m*/*z*): 2507.99 (M^+). Anal. Calcd for $C_{97}H_{55}CuF_{48}N_4O_{16}$: C, 46.45; H, 2.21; N, 2.23%. Found: C, 46.39; H, 2.25; N, 2.19%.

NMR Measurements. NMR experiments were performed at 300 K on a Bruker Avance 600 MHz with a 5 mm inverse broad-band probe equipped with *z*-axis gradients. All data were processed with TopSpin. A stock solution was prepared at an initial concentration of 5.6 μmol/L with toluene-d_8 as the solvent. Dilutions of 1:10, 1:100, 1:1000, and 1:5000 were prepared starting from the stock solution.

^1H NMR diffusion experiments were performed using the LED sequence with bipolar gradients[24] on the stock solution. The attenuation measured with this sequence is given by

$$I/I_0 = -\exp[D(\gamma_H \delta G2/\pi)^2(\Delta - \delta/3 - \tau/2)] \quad (1)$$

where I/I_0 is the normalized signal intensity, D is the diffusion coefficient, δ is the duration of the gradient pulse, γ_H is the gyromagnetic ratio of ^1H, G is the gradient strength, Δ is the diffusion time, and τ is eddy current delay. Typical acquisition parameters: recycle delay time between diffusion experiments, 3 s; Δ, 80 ms; δ, 4 ms; and τ, 5 ms.

Hydrodynamic radius (R_h) of an equivalent spherical particle was calculated using the Stokes−Einstein equation:

$$D = \frac{k_B T}{6\pi\eta R_h} \quad (2)$$

where η is the macroscopic viscosity value of the solvent, T is the absolute temperature, and k_B is the Boltzmann constant.

Electrochemical and Spectroelectrochemical Measurements. Absolute dichloromethane (CH_2Cl_2, 99.8%, EMD Chemicals Inc.) and pyridine (py, 99.8%, Sigma-Aldrich) were used for electrochemistry without further purification. Benzonitrile (PhCN) was purchased from Sigma-Aldrich and distilled over P_2O_5 under a vacuum prior to use. Tetra-*n*-butylammonium perchlorate (TBAP), used as supporting electrolyte, was purchased from Sigma-Aldrich or Fluka, recrystallized from ethyl alcohol, and dried under a vacuum at 40 °C for at least one week prior to use.

Cyclic voltammetry was carried out with an EG&G model 173 potentiostat/galvanostat. A homemade three-electrode electrochemistry cell was used consisting of a platinum button or glassy carbon working electrode, a platinum wire counter electrode, and a saturated calomel reference electrode (SCE). The SCE was separated from the bulk of the solution by a fritted-glass bridge of low porosity that contained the solvent/supporting electrolyte mixture. All potentials were referenced to the SCE.

Thin-layer UV−visible spectroelectrochemical experiments were performed with a home-built thin-layer cell that had a light transparent platinum net working electrode. Potentials were applied and monitored with an EG&G PAR Model 173 potentiostat. Time-resolved UV−visible spectra were recorded with a Hewlett-Packard Model 8453 diode array spectrophotometer. High-purity N_2 from Trigas was used to deoxygenate the solution and was kept over the solution during each electrochemical and spectroelectrochemical experiment.

RESULTS AND DISCUSSION

The formation of the triaryltetrabenzocorrole by the cross-coupling methodology involves reaction of an octabrominated copper corrolate with terminal alkenes possessing electron-withdrawing groups, as previous reported for the preparation of tetrabenzoporphyrin systems.[22] The first tetrabenzocorrole obtained by this procedure was prepared starting from the halogenated corrole **1** and methyl acrylate, leading to the formation of an annulated corrole functionalized with eight carboxymethyl moieties on the fused rings. The presence of substituents at the periphery of the macrocycle influences the optical features of this derivative as compared to the spectral properties of the unsubstituted tetrabenzocorrole.[20]

Ghosh and co-workers studied the influence of peripheral substituents on the optical spectra of copper triarylcorroles[25] and reported that a significant variation of the Soret band maxima could occur, depending upon the specific substituents present on the *meso*-phenyl rings. This result was attributed to a ligand-to-metal charge transfer transition, which was assigned as one signature of the "noninnocent" character of the corrole ligand. The assignment is also supported by the saddle structure of copper corroles, even in the absence of peripheral crowding, and results from the deviation from planarity necessary to allow a metal (dx^2-y^2)−corrole π orbital interaction. It should be noted, however, that peripheral crowding can enhance the red shifts of the Soret bands; in the case of tetrabenzocorroles, we were able to determine the structure of the copper complex of the unsubstituted 5,10,15-triphenyltetrabenzocorrole,[20] which is saddled, but the distortion was not significantly different from what is observed for other copper corrole derivatives. On the other hand, we hypothesize that the molecular structure should be significantly different in the case of tetrabenzocorroles substituted on the fused benzene rings; thus, we conducted the present study to investigate how the electronic character of the substituents influence the redox and chemical properties of the corresponding complexes.

In the present study, we have prepared and characterized five copper triaryltetrabenzocorrolates that differ in the electron-

dx.doi.org/10.1021/ic4010467 | Inorg. Chem. 2013, 52, 8834−8844

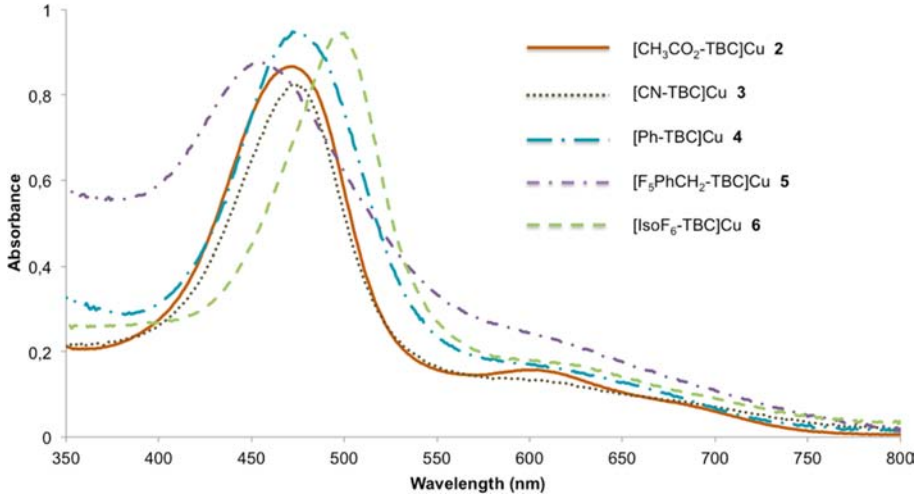

Figure 1. UV−vis spectra of the investigated tetrabenzocorroles, recorded at the following concentrations: **2** = 10.1 μM; **3** = 15.2 μM; **4** = 11.7 μM; **5** = 24.6 μM; **6** = 11.6 μM.

withdrawing groups (EWG) on the fused benzene rings. The alkene-EWG substrates chosen were cyanoacrylate, vinylbenzene, allylpentafluorobenzene, and 1,1,1,3,3,3-hexafluoroisopropylacrylate (Scheme 1). The presence of EWG is fundamental for the synthesis of benzo derivatives by the Heck cross-coupling methodology. Similar reaction conditions leading to **2**[20] have been applied to the preparation of benzocorrole derivatives **3**−**6**. Specifically, a 100-fold excess of alkene versus **1** was used in order to ensure complete bromine substitution on the corrole at 125 °C for 72 h in the presence of in situ-formed Pd(0) catalyst. Because the Heck-based route is sensitive both to the reaction time and to the temperature, as we observed during the preparation of tetrabenzocorroles bearing the $-CO_2CH_3$ moieties[20] and as reported for the case of tetrabenzoporphyrins synthesis,[22] we decided to investigate the influence of these parameters on the reaction yields. When we tried to reduce the reaction time, we noted the presence of starting material (1 h) or a complex mixture of products (1 day), indicating an incomplete conversion of the reaction intermediates to the desired tetrabenzocorrole. Reducing the temperature to 110 °C and carrying out the reaction for three days afforded a reaction mixture with spectroscopical features different from those of the tetrabenzocorrole. Taking into account the failure of these attempts, we decided to perform the preparation of **3**−**6** using the same procedure adopted for **2**. Although a certain amount of decomposition resulted from these reaction conditions, we still observed formation of the desired products in comparable yields, indicating that the different EWGs do not have a significant effect on the reactivity of the substrates when the cross-coupling reaction takes place. The overall yields for the products were always higher than 20%, a value that can be considered satisfying if we consider that the preparation of the triaryltetrabenzocorroles is a sequence of three consecutive steps. The novel benzocorroles were purified by column chromatography.

The UV−vis spectra for compounds **3**−**6** are shown in Figure 1 along with the spectrum of **2**, which was characterized in an earlier study.[23] With the exception of compound **5**, a large red shift of the Soret band is observed (in the range 40−80 nm with respect to the unsubstituted Cu triarylcorrole), whereas weak absorbances in the Q-band region of the spectra remain relatively unchanged. The spectra of **2**−**4** are quite similar to each other, whereas that of **5** and **6** are very different in terms of the position of the Soret band in CH_2Cl_2. The UV−vis spectra of **2** and **3** both have a Soret band maximum at around 474 nm, which is surprising considering the fact that the compounds display quite different electrochemistry as discussed in a later section of the manuscript.

The parent peak in the mass spectrum of **3** is assigned to the demetalated corrole, indicating a certain lability of the central metal ion in this compound (Supporting Information Figure S1); IR analysis shows a characteristic signal of the C−N triple bond at 2228 cm^{-1}. The ^{1}H NMR spectrum exhibits two main groups of signals: a broad singlet at 1.44 ppm for the *tert*-butyl groups (27 protons) and an unresolved multiplet at 7.50−7.71 ppm for the 20 aromatic protons (Supporting Information Figure S2).

Compound **4** was prepared by reacting **1** with vinylbenzene. The UV−vis spectrum of this corrole shows the Soret band at 475 nm and a single Q-band at 606 nm. The ^{1}H NMR spectrum shows resonances for the *tert*-butyl groups as a multiplet at 1.33−1.49 ppm. There is also a multiplet at 6.68−7.61 ppm for the aromatic protons (Supporting Information Figure S3). The presence of several signals for the alkyl substituents and the origin of the high-field aromatic protons of **4** with respect to **2** is likely due to aggregation phenomena. A similar behavior was recently reported for undecaarylcorroles[26] where $\pi-\pi$ interaction occurs between the *meso*-phenyl group and the two adjacent β-phenyl pyrrolic substituents or by the β-phenyl rings on the same pyrrole. The formation of the desired product is also confirmed by mass analysis, with a peak at 1568 m/z, corresponding to the molecular weight of the desired product (Supporting Information Figure S4). We also observe three other signals differing by approximately 100, 200, and 300 units from the value of the molecular peak of **4**. These signals correspond to fragmentation of the fused benzene ring followed by loss of the −C−CH−Ph unit linked to the pyrrole.

The benzocorrole **5**, obtained by reacting **1** with allylpentafluorobenzene, exhibits the most severe broadening of the absorbance bands among all the compounds investigated. The ^{1}H NMR spectrum of **5** shows three groups of signals: (1) a broad singlet at 1.41 ppm for the *tert*-butyl groups, (2) multiplets (16 H) in the range 3.47−3.53 that belong to the methylene bridge between the pentafluorophenyl groups and

dx.doi.org/10.1021/ic4010467 | *Inorg. Chem.* 2013, 52, 8834−8844

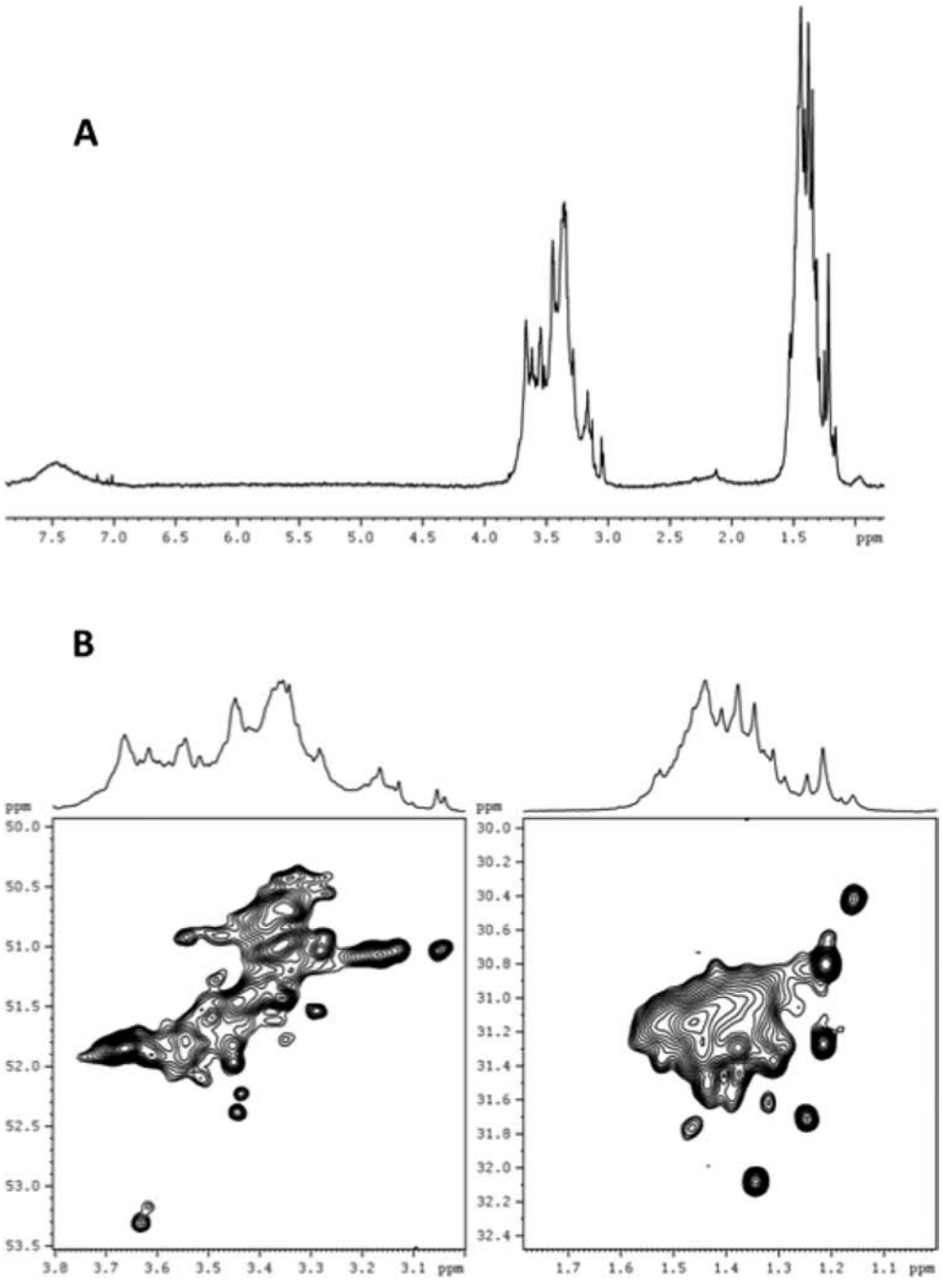

Figure 2. (A) ^{1}H NMR spectrum of **2** in toluene-d_8. (B) ^{1}H−^{13}C HSQC spectrum of **2** in toluene-d_8.

the macrocycle, and (3) the *meso*-phenyl and *β*,*β*′-fused benzene protons (Supporting Information Figure S5). The series of novel tetrabenzocorroles was completed with the preparation of **6**, obtained from **1** and 1,1,1,3,3,3-haxafluoroisopropyl acrylate. Among all the compounds synthesized, this benzocorrole shows the largest red shift of the Soret band, which is located at 498 nm. The ^{1}H NMR spectrum of this benzocorrole is characterized by its low resolution, with a multiplet at 1.39−1.45 ppm for the *tert*-butyl moieties, a multiplet at 5.76−5.98 for the hydrogen atom on the hexafluoroisopropyl substituents, and multiplets for the aromatic protons in the region 7.33−7.63 ppm (Supporting Information Figure S7).

NMR Characterization of 2. The drawback of the low-resolution NMR spectrum was earlier reported for all of the benzocorroles obtained by the cross-coupling methodology,[20,23] and it has been confirmed for the tetrabenzocorroles **3**−**6**. We decided to study this peculiarity of tetrabenzocorroles in more detail using **2** as case study to obtain more information on the behavior of these macrocycles. The choice of **2** is due to the presence of the peripheral carboxymethyl susbstituent, which afford a simplified ^{1}H NMR spectrum. In fact, compound **2** shows signals in the three expected regions of the spectrum according to its chemical structure (Figure 2A): aromatic protons show broad signals at δ around 7.5 ppm, O−CH_3 groups at 3.5 ppm, and *tert*-butyl CH_3 protons at 1.4 ppm. The integral values for the three regions are those expected for the chemical structure of **2**. However, the number of signals, particularly in the 3.5 and 1.4 ppm regions, are larger than those expected for a single molecule (4 for the O−CH_3 and 2 for the

dx.doi.org/10.1021/ic4010467 | *Inorg. Chem.* 2013, 52, 8834−8844

tert-butyl CH_3). The large number of signals can be better visualized in the $^1H-^{13}C$ HSQC spectrum (Figure 2B). The chemical shift of the carbon nuclei are very similar for the whole set of signals belonging to each region, indicating that the ^1H signals of the 3.5 and 1.4 ppm regions belong to $O-CH_3$ and *tert*-butyl CH_3 groups, respectively. A second feature of the ^1H NMR spectrum of **2** is the differential line shape observed for aromatics proton, which are much broader than the methyl protons. This fact clearly points to a dynamic equilibrium between different forms of **2** in solution. Although the large number of signals observed in the 3.5 and 1.4 regions, together with the low number of conformational freedom degrees expected for this molecule, safely excludes a conformational equilibrium, we ruled out this possibility by running variable temperature ^1H NMR experiments, registering the spectra using CD_2Cl_2 for low temperatures and toluene-d_8 for high temperature. No variations of the spectral features were observed in the temperature range compatible with solvents used. This fact leaves molecular association as the only possible explanation for the heterogeneity of signals observed.

In order to further explore this possibility, ^1H NMR spectra were acquired after successive dilutions of the sample (Figure 3). As can be observed for the 3.5 ppm region, there are changes in the chemical shift of the signals and the number of signals detected with concentration.

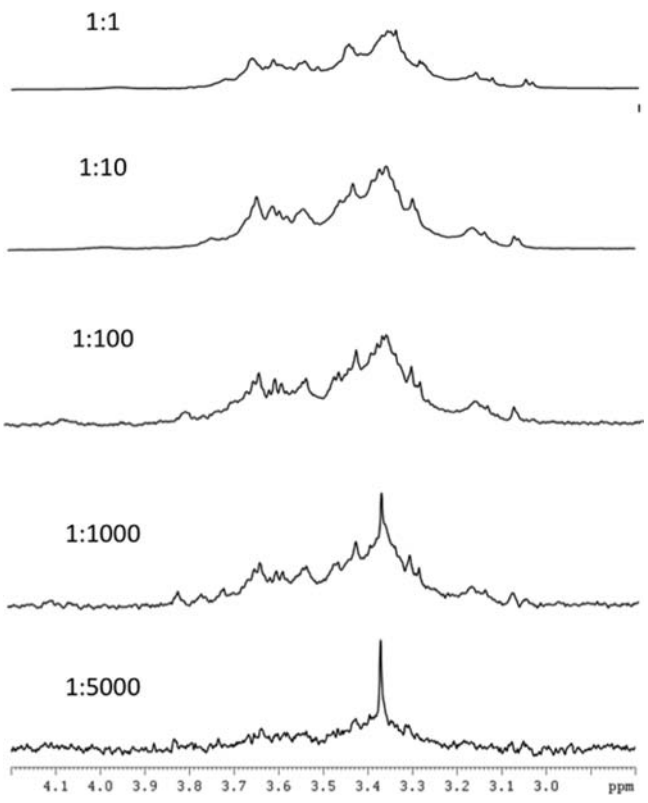

Figure 3. ^1H NMR spectra of **2** in toluene-d_8 at different dilutions ($-OCH_3$ groups region).

In the most dilute condition, a single signal is emerging, probably belonging to the monomeric molecule. Similar behavior was observed in the 1.4 ppm region (data not shown). On the other hand, aromatic signals were not detectable at low concentrations, probably due to a residual broadening.

To further characterize the mixture present in solution at the highest concentration, we have measured the self-diffusion coefficients by gradient-pulsed NMR experiments using different signals in the 3.5 and 1.4 ppm regions. The values are reported in Table 1. These values are used in the Stokes–Einstein equation (eq 2) to extract the size of the solute molecules treated as Brownian particles of spherical shape.[27] The calculated hydrodynamic radius (R_h) corresponds to an equivalent spherical particle showing the same hydrodynamic behavior as that of the solute molecule. The calculated R_h values are also indicated in Table 1.

Table 1. Self-Diffusion Coefficients (D) Measured at 300 K in Toluene for Compound 2 and the Calculated Hydrodynamic Radius for Different Signals in the 3.5 and 1.4 ppm Region

δ (ppm)	$D/10^{-10}$ (m^2/s)	R_h (nm)
1.159	4.45	0.91
1.217	4.69	0.86
1.247	4.71	0.86
1.290	4.85	0.84
1.311	4.82	0.84
1.329	4.97	0.82
1.346	4.84	0.84
1.377	4.80	0.85
3.039	4.38	0.93
3.291	6.94	0.58
3.343	6.08	0.67
3.354	5.66	0.72
3.374	5.63	0.72
3.517	4.97	0.82
3.616	4.72	0.86
3.663	4.75	0.85

A comparison between the extracted value of the equivalent hydrodynamic radius and the actual molecular size of **2** can be performed if the molecular shape of this type of molecules is used. On the basis of several crystallographic structures of corrole compounds, a single molecule of **2** can be described as a disk with a height (l) of 0.3 nm and a diameter (d) of 1.6 nm. Equation 3 can be used to define the relationship between R_h and the height-to-diameter radio, $p = l/d$:[28]

$$\frac{R_h}{l} = \frac{1}{2}p^{-2/3}[a_1 + a_2(\ln p) + a_3(\ln p)^2 + a_4(\ln p)^3] \quad (3)$$

with $0.1 \leq p \leq 20$, and

$$a_1 = 1.155; \quad a_2 = 1.597 \times 10^{-2}; \quad a_3 = 9.020 \times 10^{-2}; \quad a_4 = 6.914 \times 10^{-3} \quad (4)$$

Associations of two, three, or four molecules form disks with different heights but approximately equal diameters. When the interaction of two molecules in the asymmetric cell of crystal structures of corrole molecules is analyzed, one can assume that each molecule added on the top will increase the height by 0.4 nm. Equation 3, when applied to these different molecular associations, yields R_h values ranging from 0.6 to 0.9 nm (Table 2). Comparison of the calculated R_h values from the NMR signals in Table 1 with those expected for different associations between one and four molecules of **2** produces a picture that explains the high number of signals observed in the proton

dx.doi.org/10.1021/ic4010467 | Inorg. Chem. 2013, 52, 8834–8844

Table 2. Equivalent Hydrodynamic Radius (R_h) for Different Molecular Associations of Compound 2, Considered As a Disk-Like Particle with Diameter d = 1.6 nm

number of associated molecules	l (nm)	p	R_h (nm)
1	0.3	0.19	0.62
2	0.7	0.44	0.73
3	1.1	0.69	0.82
4	1.5	0.94	0.90

NMR spectrum (Figure 1) and the signal simplification that correlates with sample dilution (Figure 2). Compound **2** exists at high concentrations as a complex mixture of different molecules associated in equilibrium. In the case of three and four associated molecules, it is likely that there is more than one type of molecular orientation within the complex, leading to different chemical shifts for the ^{1}H nuclei. The value of the exchange kinetic constant is of the same order of magnitude as the chemical shift difference for aromatic protons, leading to severe broadening. It is possible that the difference for the chemical shift of methyl protons is even larger, leading to a slow exchange scenario in which separated signals are observed.

Electrochemistry and Spectroelectrochemistry. Electrochemical and spectroscopic studies of triphenylcorroles (TPC) containing electron-donating or electron-withdrawing substituents on the *meso* and/or *β*-pyrrolic positions of the macrocycle have been investigated in detail.[29−35] The electrochemistry of the ring-expanded corrole **2**, was earlier described in the literature,[23] and the redox properties of four newly synthesized ring-expanded corroles that have different electron-withdrawing substituents on the fused benzene rings of the tetrabenzocorrole are examined in the present study.

Cyclic voltammograms illustrating the oxidations and reductions of compounds **3**−**6** in CH_2Cl_2, 0.2 M TBAP, and PhCN are shown in Figure 4, whereas cyclic voltammograms in pyridine and 0.2 M TBAP are given in Supporting Information Figure S9. The measured half-wave or peak potentials are summarized in Table 3, which includes previously published data for compound **2**.[23] The proposed site of electron transfer for each redox reaction (conjugated ring system, metal center, or fused benzene ring) is also given in the table, with these assignments being based on the measured spectral changes, measured $E_{1/2}$ values, and previous assignments of the electron transfer site reported in the literature for related compounds.[23,34,35]

As shown in Table 3 and Figure 4, the investigated tetrabenzocorroles can undergo two reversible or quasi-reversible one-electron oxidations in CH_2Cl_2 or PhCN, the first of which is located at $E_{1/2}$ values between 0.57 and 1.06 V versus the SCE, and the second of which is between 1.09 and 1.59 V.

The exact number of observed oxidations, as well as the measured redox potentials, will depend upon the electron-

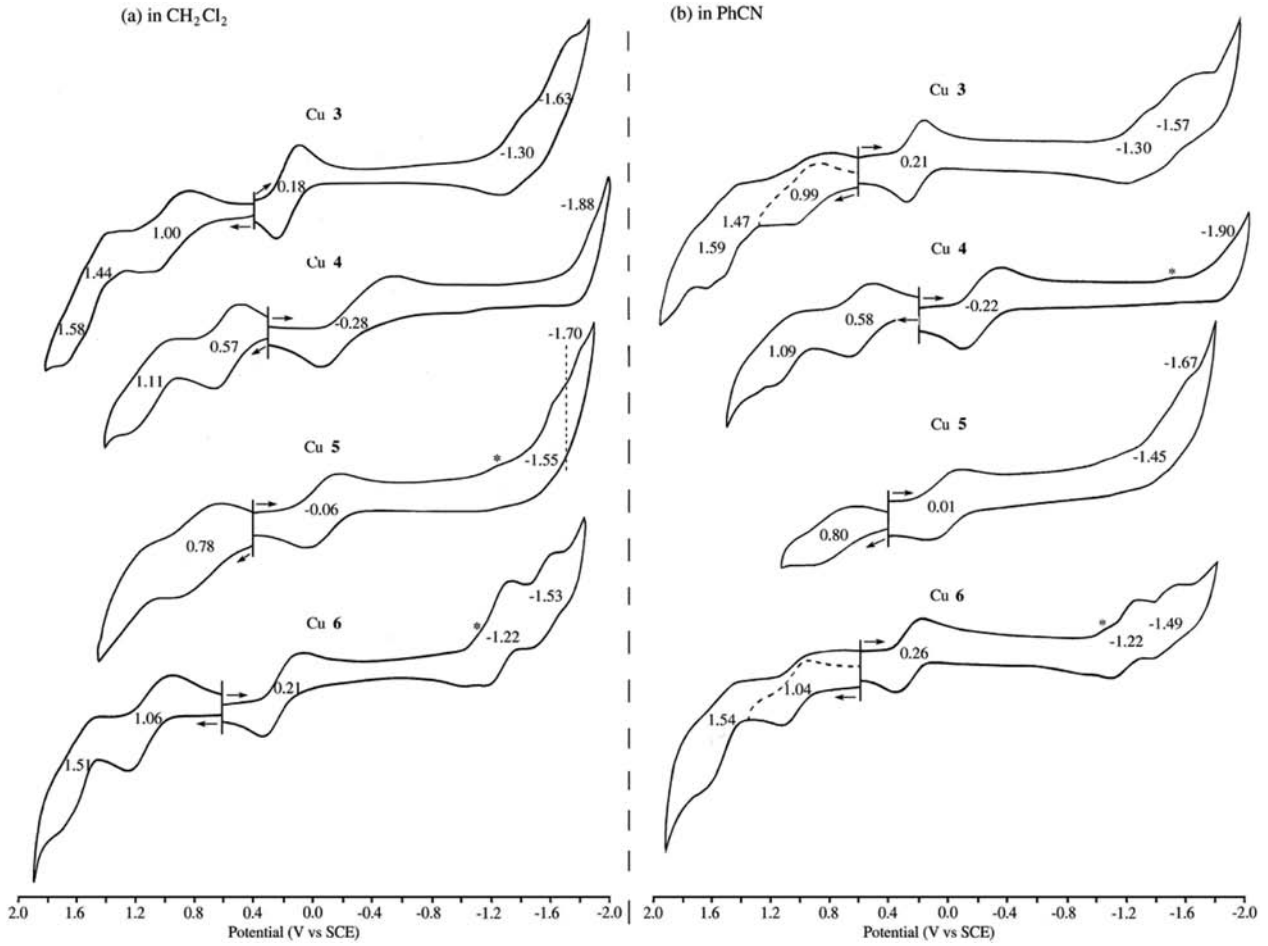

Figure 4. Cyclic voltammograms of (TBC)Cu derivatives (**3**−**6**) in CH_2Cl_2 and PhCN containing 0.2 M TBAP at scan rate of 0.1 V/s. Some small reduction peaks, marked by asterisks, are probably due to unstable reduced products.

dx.doi.org/10.1021/ic4010467 | Inorg. Chem. 2013, 52, 8834−8844

Table 3. Cyclic Voltammetry of (TBC)Cu Derivatives in CH_2Cl_2, PhCN, and Pyridine Containing 0.2 M TBAP at a Scan Rate of 0.1 V/s

		oxidation		reduction		
solvent	compound	2nd ring	1st ring	1st Cu^{III}/Cu^{II}	2nd benzo-x^a	3rd ring
CH_2Cl_2	Cu **2**[b]	1.38	0.82	0.07	−1.38	−1.59
	Cu **3**	1.58, 1.44	1.00	0.18	−1.30	−1.63
	Cu **4**	1.11	0.57	−0.28		−1.88[d]
	Cu **5**		0.78	−0.06	−1.55[c]	−1.70
	Cu **6**	1.51	1.06	0.21	−1.22[c]	−1.53
PhCN	Cu **2**[b]	1.39	0.80	0.06	−1.42	−1.62
	Cu **3**	1.59, 1.47	0.99	0.21	−1.30	−1.57
	Cu **4**	1.09	0.58	−0.22		−1.90[d]
	Cu **5**		0.81	0.01	−1.45	−1.67[b]
	Cu **6**	1.54	1.04	0.26	−1.22[c,d]	−1.49
Pyridine	Cu **2**[b]		0.71	0.11	−1.33	−1.55
	Cu **3**		0.75	0.25	−1.46[c,d]	−1.66[d,e]
	Cu **4**		0.54	−0.20		−1.86
	Cu **5**		0.74[d]	0.04	−1.46[c,d]	−1.60[d]
	Cu **6**		1.05[d]	0.23	−1.17[b]	−1.48[e]

[a]The fused benzene ring with electron-withdrawing substituents does not participate in conjugated system of the macrocycle. [b]Data is taken from ref 23. [c]Some small reduction peaks are seen at E_p = −1.04 to −1.25 V due to trace impurities or side reactions (see Figure 4). [d]Peak potential at a scan rate of 0.1 V/s. [e]Additional reduction observed between −1.75 and −1.88 V.

withdrawing properties of the fused phenyl ring substituents and the specific solvent. In all cases, however, the products of these two oxidations are a corrole π−cation radical in the first step and a corrole dication in the second. Only the first oxidation can be detected in pyridine, due to the limited positive potential window of this solvent.

A second oxidation of **5** is not observed in CH_2Cl_2 or PhCN, implying that the generated radical cation of this compound is unstable in these two solvents. Moreover, as is seen in Figure 4, the second oxidation of **3** is split into two processes, one at $E_{1/2}$ = 1.44−1.47 V and the other at 1.58−1.59 V, depending upon the solvent. The splitting of the second oxidation into two processes can be accounted for by aggregation or dimerization of the tetrabenzocorrole after the abstraction of one electron.

Three major reductions can be detected for compounds **2**, **3**, **5**, and **6**. The first involves a Cu^{III}/Cu^{II} process, whereas the second is assigned to occur at one of the four fused benzene rings whose reduction is made easier by the presence of the electron-withdrawing substituent. The fused benzene ring that is reduced does not participate in the conjugated π system of the macrocycle; thus, the potentials for this electron addition should be quite close to $E_{1/2}$ values for the reduction of a monosubstituted benzene with the same electron-withdrawing group.

One example of this is seen in the case of $C_6H_4(CN)_2$, whose reduction occurs at about −1.30 V in CH_3CN[38] as compared to an $E_{1/2}$ of −1.30 V for compound **3** in PhCN (see Table 3).

Compound **4**, which contains weakly electron-withdrawing phenyl substituents, does not undergo a reduction at the fused benzene ring and has behavior typical of what has been reported for numerous corroles with a "regular" macrocycle.[35] The third reduction of **2**, **3**, **5**, and **6** is assigned as occurring at the π ring system of the tetrabenzocorrole, as is the second reduction of **4**. These ring-centered reductions are all relatively close to the negative potential limit of the solvent and are quasi-reversible or irreversible in some cases. Additional ill-defined reductions with small peak currents are also observed for some of the compounds (this is especially evident for **3** and **5** in pyridine). In CH_2Cl_2 or PhCN, the unknown side reactions are indicated by an asterisk in the cyclic voltammograms of Figure 4 and are assigned as due to a reduction of trace side products generated under the given solution conditions.

The electroreductions and electrooxidation of **3**−**6** were also characterized by UV−visible thin-layer spectroelectrochemistry. Examples of the UV−visible spectral changes that occur during the first two oxidations of **3** and **6** in PhCN are illustrated in Figure 5. For both compounds, the spectral transitions between the neutral and singly or doubly oxidized species are consistent with macrocycle-centered electron transfer processes of porphyrin-like molecules.[36] The similar final spectrum obtained after the second split oxidation of **3** and the unsplit oxidation of **6** (see cyclic voltammograms in Figure 4) suggests that the "extra" oxidation process of **3** at $E_{1/2}$ = ∼1.59 V in the cyclic

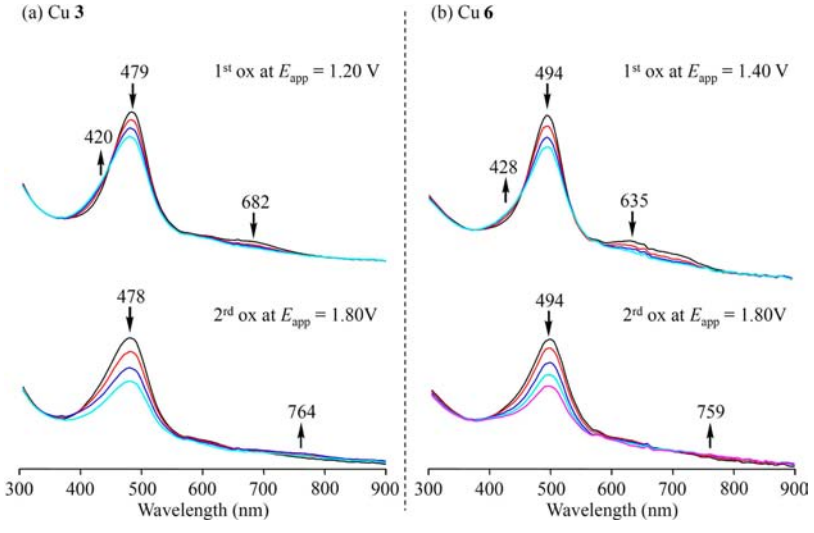

Figure 5. Thin-layer UV−vis spectral changes of (a) Cu **3** and (b) Cu **6** in PhCN containing 0.2 M TBAP during the indicated oxidations.

dx.doi.org/10.1021/ic4010467 | Inorg. Chem. 2013, 52, 8834−8844

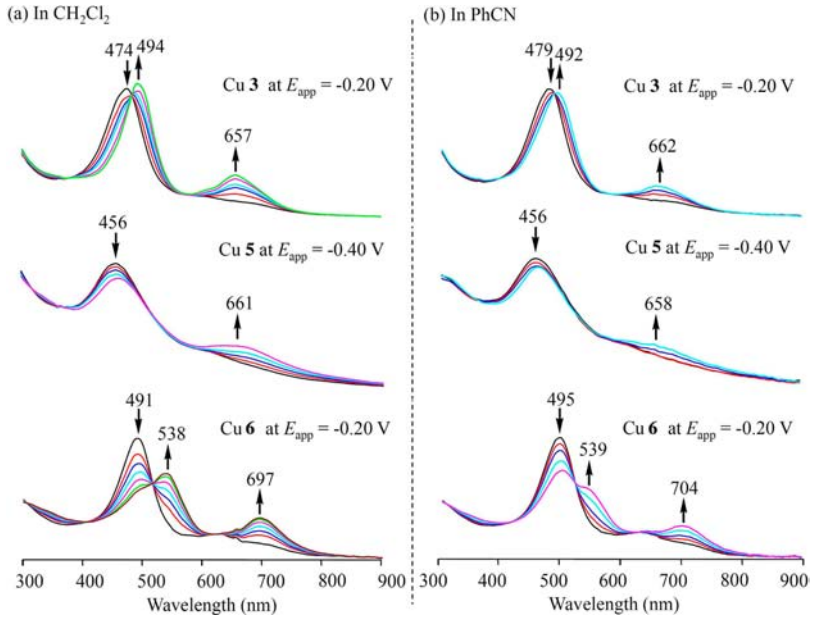

Figure 6. Thin-layer UV−vis spectral changes of $Cu^{III/II}$ reduction for the investigated Cu compounds **3**, **5**, and **6** in (a) CH_2Cl_2 and (b) PhCN containing 0.2 M TBAP.

voltammograms is associated with aggregation or dimerization and does not effect the final product of the two-electron abstraction to give a tetrabenzocorrole dication.

As shown in Figure 6, three different kinds of spectral changes are seen for the first one-electron reduction of compounds **3**, **5**, and **6** in PhCN or CH_2Cl_2. The first is for compound **3**, which exhibits a 13−20 nm shift in the position of the Soret band and a moderate intensity shift of the Q-band at 657−662 nm upon conversion of Cu^{III} to Cu^{II}. The second is for compound **5**, which exhibits a decreased intensity of the Soret band during the metal centered reduction but only small changes in the wavelength of maximum absorbance. The third type of spectral change is for compound **6**, which exhibits a substantial shift in the Soret band position along with a large decrease in intensity of the band after reduction of Cu^{III} to Cu^{II}.

The relative intensities of the Soret bands for the Cu^{II} form of the tetrabenzocorrole are quite different from each other, probably due to a difference in aggregation between the two compounds. On the other hand, the visible band at 657−704 nm is common to all three compounds. A similar difference in the types of spectra was observed in our previous study of Cu β-nitrocorroles[35] and was proposed to involve an equilibrium between a Cu^{II} corrole and a Cu^{III} corrole π-anion radical product in the first reduction process.[32−35,37−40] Spectral changes of **2** and **4** for this process are similar to those of **3**.

The spectral changes that occur for compound **3** in PhCN during the second and third controlled potential reductions are given in Supporting Information Figure S10. The spectral changes obtained during the first one-electron addition are similar to what was reported in our previous study of compound **2**,[23] but only minimal changes are observed in the spectrum of the Cu^{II} corrole during the second electron addition, which we have assigned as the reduction of one benzene−CN group on the compound. Potentials have been reported in the literature for electroreduction of benzenes with one- or two-electron-withdrawing groups (e.g., −CN,[41] $-NO_2$, −Br, and −COOMe[42,43]), and these values are consistent with reduction potentials measured in the present study for compounds **2**, **3**, **5**, and **6** under similar solution conditions. Consistent with our assigned reduction of a fused phenyl ring in the second reduction process, the spectral changes recorded for **3** during the third one-electron reduction resemble what is expected for a macrocycle-centered electron transfer.

The measured $E_{1/2}$ values of **2**−**6** shift positively or negatively with changes in the electron-withdrawing character of the substituents at the four fused benzene rings of the macrocycle. The relevant electrochemical linear free energy relationship is given by the equation $\Delta E_{1/2} = 4\sigma\rho$, where the substituent constant, σ, provides a measure of the electron-withdrawing characteristics of the substituent and ρ, the "reaction constant", indicates the magnitude of the interactions; the larger the value of ρ, the larger the substituent effect.[44−46] The values of 4σ for **2** (COOMe), **3** (CN), and **4** (C_6H_5) are 3.28, 4.88, and 0.20, respectively, obtained from ref 41.

Substituent constants are not available for compounds **5** and **6**, but correlations between $E_{1/2}$ for the first oxidation and first reduction of compounds **2**−**4** give a linear slope as seen in Figure 7. The slopes (ρ) of 90−100 mV indicate that these three compounds follow the same linear free energy relationship and, thus, undergo the same electron transfer mechanism during the first oxidation and first reduction under the given experimental conditions. The $\Delta E_{1/2}$ between the first reduction and first oxidation of compounds **2**−**4** ranges from 0.75 to 0.85 V, and a similar $\Delta E_{1/2}$ is seen for compounds **5** (0.84 V) and **6** (0.85 V) in CH_2Cl_2.

■ CONCLUSIONS

The scope of the synthetic route to obtain tetrabenzocorroles via a Heck cross-coupling reaction is quite general when the alkene used in the reaction bears an electron-withdrawing substituent. Using this route, we have successfully prepared different tetrabenzocorrole Cu complexes bearing electron-withdrawing groups at the β-fused benzene rings. The spectroscopic and electrochemical characterization of these macrocycles gave some insights on the influence of such substituents on the properties of the corresponding tetraben-

dx.doi.org/10.1021/ic4010467 | Inorg. Chem. 2013, 52, 8834−8844

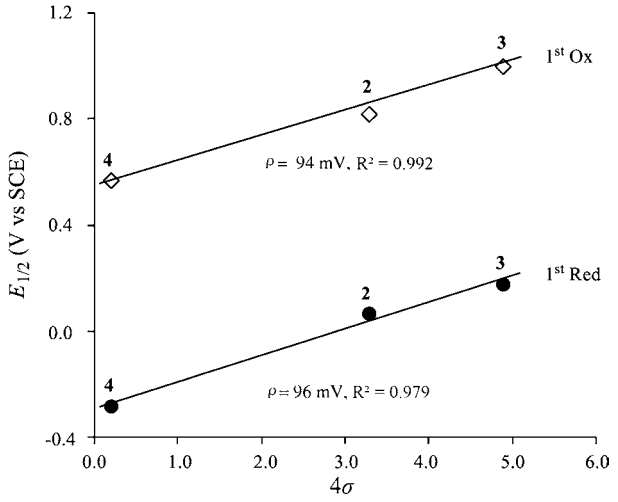

Figure 7. Correlation between half-wave potential ($E_{1/2}$) in CH_2Cl_2 for the first oxidation and first reduction of **2**–**4** vs substituent constants (4σ) on the fused benzene ring.

zocorrole–Cu complexes. The NMR characterization showed a strong tendency of these macrocycles to aggregate in solution, resulting in a significant line broadening of the spectra. This effect is also reflected in the UV–vis spectral features, where only slight modifications have been observed in the spectroscopic features of the functionalized tetrabenzocorroles, which is probably due to the band broadening induced by aggregation. On the other hand, the electrochemistry showed a good linear correlation of the first oxidation and first reduction processes with the electron-withdrawing characteristics of the substituents. An additional reduction process is present for all of the examined compounds as compared to what is usually observed for Cu corrole complexes; this reduction can be attributed to the fused benzene rings bearing highly electron-withdrawing substituents and is not present in the case of compound **4**, which has only weakly electron-withdrawing phenyl substituents.

The quite general scope of the synthetic route allows the possibility of tuning the properties of these macrocycles, an important step for their practical application in different fields, an example of which is in the area of catalysis or chemical sensors. Among the different tetrabenzocorroles reported, compound **2** is particularly interesting because hydrolysis of the carboxymethyl groups makes this corrole soluble in water solutions, opening the way to the exploitation of this class of compounds in biological systems. This study is currently under investigation in our laboratories, and the results will be presented in the future.

■ ASSOCIATED CONTENT

Ⓢ Supporting Information

Mass and ^{1}H NMR spectra, CVs of **3**–**6**, and UV–vis spectral changes of **3** during applied potentials. This material is available free of charge via the Internet at http://pubs.acs.org.

■ AUTHOR INFORMATION

Corresponding Author

*E-mail: roberto.paolesse@uniroma2.it.

Notes

The authors declare no competing financial interest.

■ ACKNOWLEDGMENTS

The authors thank the Italian MIUR (R.P., PRIN2009 project 2009Z9ASCA) and the Robert A. Welch Foundation (K.M.K., Grant E-680) for financial support.

■ REFERENCES

(1) Johnson, A. W.; Kay, I. T. *J. Chem. Soc.* **1965**, 1620.
(2) Gross, Z.; Galili, N.; Saltsman, I. *Angew. Chem., Int. Ed.* **1999**, *38*, 1427–1429.
(3) Paolesse, R.; Jaquinod, L.; Nurco, D. J.; Mini, S.; Sagone, F.; Boschi, T.; Smith, K. M. *Chem. Commun.* **1999**, 1307–1308.
(4) Paolesse, R.; Marini, A.; Nardis, S.; Froiio, A.; Mandoj, F.; Nurco, D. J.; Prodi, L.; Montalti, M.; Smith, K. M. *J. Porphyrins Phthalocyanines* **2003**, *7*, 25–36.
(5) Gryko, D.; Koszarna, B. *Org. Biomol. Chem.* **2003**, *1*, 350–357.
(6) Koszarna, B.; Gryko, D. *J. Org. Chem.* **2006**, *71*, 3707–3717.
(7) Paolesse, R. *Synlett* **2008**, *15*, 2215–2230.
(8) Aviv-Harel, I.; Gross, Z. *Chem.—Eur. J.* **2009**, *15*, 8382–8394.
(9) Lemon, C. M.; Brothers, P. J. *J. Porphyrins Phthalocyanines* **2011**, *15*, 809–834.
(10) Kupershmidt, L.; Okun, Z.; Amit, T.; Mandel, S.; Saltsman, I.; Mahammed, A.; Bar-Am, Z.; Gross, Z.; Youdim, M. B. H. *J. Neurochem.* **2010**, *113*, 363–373.
(11) Tortora, L.; Pomarico, G.; Nardis, S.; Martinelli, E.; Catini, A.; D'Amico, A.; Di Natale, C.; Paolesse, R. *Sens. Actuators, B* **2013**, No. 10.1016/j.snb.2012.09.055.
(12) Walker, D.; Chappel, S.; Mahammed, A.; Brunschwig, S.; Winkler, J. R.; Gray, H. B.; Zaban, Z.; Gross, Z. *J. Porphyrins Phthalocyanines* **2006**, *10*, 1259–1262.
(13) Carvalho, C. M. B.; Brocksom, T. J.; de Oliveira, K. T. *Chem. Soc. Rev.* **2013**, *42*, 3302–3317.
(14) Finikova, O. S.; Aleshchnkov, S. E.; Briñas, R. P.; Cheprakov, A. V.; Carroll, P. J.; Vinogradov, S. A. *J. Org. Chem.* **2005**, *70*, 4617–4628.
(15) Filatov, M. A.; Baluschev, S.; Ilieva, I. Z.; Enkelmann, V.; Miteva, T.; Landfester, K.; Aleshchnkov, S. E.; Cheprakov, A. V. *J. Org. Chem.* **2012**, *77*, 11119–11131.
(16) Xu, H.-J.; Mack, J.; Descalzo, A. B.; Shen, Z.; Kobayashi, N.; You, X.-Z.; Rurack, K. *Chem.—Eur. J.* **2011**, *17*, 8965–8983.
(17) Spencer, J. D.; Lash, T. D. *J. Org. Chem.* **2000**, *65*, 1530–1539.
(18) Lash, T. D. *J. Porphyrins Phthalocyanines* **2001**, *5*, 267–288.
(19) Lebedev, A. Y.; Filatov, M. A.; Cheprakov, A. V.; Vinogradov, S. A. *J. Phys. Chem. A* **2008**, *112*, 7723–7733.
(20) Pomarico, G.; Nardis, S.; Paolesse, R.; Ongayi, O. C.; Courtney, B. H.; Fronczek, F. R.; Vicente, M. G. H. *J. Org. Chem.* **2011**, *76*, 3765–3773.
(21) Finikova, O. S.; Cheprakov, A. V.; Beletskaya, I. P.; Carroll, P. J.; Vinogradov, S. A. *J. Org. Chem.* **2004**, *69*, 522–535.
(22) Deshpande, R.; Jiang, L.; Schmidt, G.; Rakovan, J.; Wang, X.; Wheeler, K.; Wang, H. *Org. Lett.* **2009**, *11*, 4251–4253.
(23) Pomarico, G.; Nardis, S.; Naitana, M. L.; Vicente, M. G. H.; Kadish, K. M.; Chen, P.; Prodi, L.; Genovese, D.; Paolesse, R. *Inorg. Chem.* **2013**, *52*, 4061–4070.
(24) Wu, D.; A. Chen, A.; Johnson, C.S. J. *J. Magn. Reson., Ser. A* **1995**, *115*, 260–264.
(25) Wasbotten, I. H.; Wondimagegn, T.; Ghosh, A. *J. Am. Chem. Soc.* **2002**, *124*, 8104–8116.
(26) Gao, D.; Canard, G.; Giorgi, M.; Balaban, T. S. *Eur. J. Inorg. Chem.* **2012**, 5915–5920.
(27) Robinson, R. A.; Stokes, R. H. *Electrolyte Solutions*, 2nd ed.; Butterworth: London, 1959.
(28) Ortega, A.; García de la Torre, J. *J. Chem. Phys.* **2003**, *119*, 9914–9919.
(29) Will, S.; Lex, J.; Vogel, E.; Schmickler, H.; Gisselbrecht, J. P.; Haubtmann, C.; Bernard, M.; Gross, M. *Angew. Chem., Int. Ed. Engl.* **1997**, *36*, 357–361.
(30) Guilard, R.; Barbe, J.-M.; Stern, C.; Kadish, K. M. In *The Porphyrin Handbook*; Kadish, K. M., Smith, K. M., Guilard, R., Eds.; Academic Press: San Diego, 2000; Vol. *18*, pp 303–349.

(31) Guilard, R.; Gros, C. P.; Barbe, J. M.; Espinosa, E.; Jerome, F.; Tabard, A.; Latour, J. M.; Shao, J.; Ou, Z.; Kadish, K. M. *Inorg. Chem.* **2004**, *43*, 7441−7455.
(32) Bruckner, C.; Brinas, R. P.; Bauer, J. A. *Inorg. Chem.* **2003**, *42*, 4495−4497.
(33) Luobeznova, I.; Simkhovich, L.; Goldberg, I.; Gross, Z. *Eur. J. Inorg. Chem.* **2004**, 1724−1732.
(34) Ou, Z.; Shao, J.; Zhao, H.; Ohkubo, K.; Wasbotten, I. H.; Fukuzumi, S.; Ghosh, A.; Kadish, K. M. *J. Porphyrins Phthalocyanines* **2004**, *8*, 1236−1247.
(35) Stefanelli, M.; Mandoj, F.; Mastroianni, M.; Nardis, S.; Mohite, P.; Fronczek, F. R.; Smith, K. M.; Kadish, K. M.; Xiao, X.; Ou, Z.; Chen, P.; Paolesse, R. *Inorg. Chem.* **2011**, *50*, 8281−8292.
(36) Chen, P.; Finikova, O. S.; Ou, Z.; Vinogradov, S. A; Kadish, K. M. *Inorg. Chem.* **2012**, *51*, 6200−6210.
(37) Kadish, K. M.; Adamian, V. A.; Van-Caemelbecke, E.; Gueletii, E.; Will, S.; Erben, C.; Vogel, E. *J. Am. Chem. Soc.* **1998**, *120*, 11986−11993.
(38) Alemayehu, A. B.; Gonzalez, E.; Hansen, L. K.; Ghosh, A. *Inorg. Chem.* **2009**, *48*, 7794−7799.
(39) Oort, B. V.; Tangen, E.; Ghosh, A. *Eur. J. Inorg. Chem.* **2004**, 2442−2445.
(40) Bröring, M.; Brégier, F.; Tejero, E. C.; Hell, C.; Holthausen, M. C. *Angew. Chem., Int. Ed.* **2007**, *46*, 445−448.
(41) Sertel, M.; Yildiz, A.; Gambert, R.; Baumgärtel, H. *Electrochim. Acta* **1986**, *31*, 1287−1292.
(42) In *Organic Electrochemistry*, 4th ed.; Hammerich, O., Lund, H., Eds.; Marcel Dekker: New York, 2000; pp 453−471.
(43) Fox, M. A. In *Topics in Organic Electrochemistry*; Fry, A. J., Britton, W. E., Eds.; Plenum Press: New York, 1986; pp 199−200.
(44) Hansch, C.; Leo, A.; Taft, R. W. *Chem. Rev.* **1991**, *91*, 165−195.
(45) Kadish, K. M.; Morrison, M. M. *J. Am. Chem. Soc.* **1976**, *98*, 3326−3328.
(46) Kadish, K. M.; Morrison, M. M.; Constant, L. A.; Dickens, L.; Davis, D. D. *J. Am. Chem. Soc.* **1976**, *98*, 8387−8390.